HHS Public Access

Author manuscript

Nat Commun. Author manuscript; available in PMC 2013 January 03.

Published in final edited form as:

Nat Commun. ; 3: 937. doi:10.1038/ncomms1938.

Reprogramming of tRNA modifications controls the oxidative stress response by codon-biased translation of proteins

Clement T.Y. Chan[1,2], **Yan Ling Joy Pang**[1], **Wenjun Deng**[1], **I. Ramesh Babu**[1], **Madhu Dyavaiah**[3], **Thomas J. Begley**[3], and **Peter C. Dedon**[1,4,*]

[1]Department of Biological Engineering, Massachusetts Institute of Technology, Cambridge, MA 02139

[2]Department of Chemistry, Massachusetts Institute of Technology, Cambridge, MA 02139

[3]College of Nanoscale Science and Engineering, University at Albany, SUNY, Albany, NY 12203

[4]Center for Environmental Health Sciences, Massachusetts Institute of Technology, Cambridge, MA 02139

Abstract

Selective translation of survival proteins is an important facet of the cellular stress response. We recently demonstrated that this translational control involves a stress-specific reprogramming of modified ribonucleosides in tRNA. Here we report the discovery of a step-wise translational control mechanism responsible for survival following oxidative stress. In yeast exposed to hydrogen peroxide, there is a Trm4 methyltransferase-dependent increase in the proportion of $tRNA^{LEU(\underline{C}AA)}$ containing m^5C at the wobble position, which causes selective translation of mRNA from genes enriched in the TTG codon. Of these genes, oxidative stress increases protein expression from the TTG-enriched ribosomal protein gene *RPL22A*, but not its unenriched paralog. Loss of either *TRM4* or *RPL22A* confers hypersensitivity to oxidative stress. Proteomic analysis reveals that oxidative stress causes a significant translational bias toward proteins coded by TTG-enriched genes. These results point to stress-induced reprogramming of tRNA modifications and consequential reprogramming of ribosomes in translational control of cell survival.

*Corresponding author: PCD, Department of Biological Engineering, NE47-277, Massachusetts Institute of Technology, 77 Massachusetts Avenue, Cambridge, MA 02139; tel 617-253-8017; fax 617-324-7554; pcdedon@mit.edu.

AUTHOR CONTRIBUTIONS

All authors contributed to experimental design, data analysis and interpretation, and preparation of the manuscript. C.T.Y.C., Y.L.J.P., W.D. and M.D. contributed to performance of experiments.

The authors declare no competing financial interest.

Accession codes

The proteomics data have been deposited in the XX database under the XX accession code.

INTRODUCTION

Decades of study have revealed more than 100 ribonucleoside structures incorporated as post-transcriptional modifications mainly in tRNA and rRNA, with 25–35 modifications present in any one organism[1–4]. In general, tRNA modifications enhance ribosome binding affinity, reduce misreading, and modulate frame-shifting, all of which affect the rate and fidelity of translation[5–8]. Emerging evidence points to a critical role for tRNA and rRNA modifications in the various cellular responses to stimuli, such as tRNA stability[9,10], transcription of stress response genes[11–13], and control of cell growth[14].

We recently used high-throughput screens and targeted analyses to show that the tRNA methyltransferase 9 (Trm9) modulates the toxicity of methylmethanesulfonate (MMS) in *Saccharomyces cerevisiae*[12,15]. This is similar to the observed role of Trm9 in modulating the toxicity of ionizing radiation[16] and of Trm4 in promoting viability after methylation damage[15,17]. Trm9 catalyzes the methyl esterification of the uracil-based cm^5U and cm^5s^2U to mcm^5U and mcm^5s^2U, respectively, at the wobble positions of $tRNA^{UCU}_{}$-ARG and $tRNA^{UUC}_{}$-GLU, among others[18]. These wobble base modifications enhance binding of the anticodon with specific codons in mixed codon boxes[19]. Codon-specific reporter assays and genome-wide searches revealed that Trm9-catalyzed tRNA modifications enhanced the translation of AGA- and GAA-rich transcripts that functionally mapped to processes associated with protein synthesis, metabolism, and stress signalling[12]. These results lead to a model in which mRNA possessing specific codons will be more efficiently translated by tRNA with anticodons containing the Trm9-modified ribonucleoside and that tRNA modifications can dynamically change in response to stress.

To study the functional dynamics of this conserved system, we recently developed a bioanalytical platform to quantify the spectrum of ribonucleoside modifications and we used it to assess the role of RNA modifications in the stress response of *S. cerevisiae*[20]. This approach led to the discovery of signature changes in the spectrum of tRNA modifications in the cellular response to mechanistically different toxicants. Exposure of yeast to hydrogen peroxide (H_2O_2), as a model oxidative stressor, led to increases in the levels of 2′-*O*-methylcytosine (Cm), 5-methylcytosine (m^5C), and N^2,N^2-dimethylguanosine (m^2_2G), while these ribonucleosides decreased or were unaffected by exposure to MMS, arsenite, and hypochlorite[20]. Loss of the methyltransferase enzymes catalyzing the formation of the modified ribonucleosides led to cytotoxic hypersensitivity to H_2O_2 exposure[20]. These results support a general model of dynamic control of tRNA modifications in cellular response pathways and expand the repertoire of mechanisms controlling translational responses in cells.

In this present study we have used a variety of bioanalytical and bioinformatic approaches to define a step-wise mechanistic link between tRNA modifications and the oxidative stress response. Following an oxidative stress, reprogramming of a specific tRNA wobble modification leads to selective translation of mRNA species enriched with the cognate codon. Among the codon-biased, selectively translated proteins is one member of a pair of ribosomal protein paralogs, and the loss of this paralog causing sensitivity to oxidative stress. These results lead to a model in which stress-induced reprogramming of tRNA

modifications and the associated reprogramming of ribosomes provides translational control of cell survival following an oxidative stress.

RESULTS

H_2O_2 increases m^5C at the wobble position of $tRNA^{Leu(CAA)}$

In *S. cerevisiae*, m^5C is synthesized by Trm4 methyltransferase (also called Ncl1) and we previously observed that the level of m^5C in total tRNA increased following exposure to H_2O_2[20], with loss of Trm4 causing hypersensitivity to the cytotoxic effects of H_2O_2[20]. To rule out second site mutations as the cause of this phenotype, we performed a complementation study using a *TRM4* expression vector in the *trm4* mutant strain and observed that re-expression of Trm4 conferred resistance to H_2O_2 exposure (Supplementary Figure S1 and Supplementary Methods).

Though m^5C is present in at least 34 species of tRNA[2], $tRNA^{Leu(CAA)}$ is the only tRNA with m^5C at the anticodon wobble position 34, as well as position 48 at the junction between the variable and TΨC loops[2]. To determine if H_2O_2 exposure altered the levels of m^5C at one or both of these positions, $tRNA^{Leu(CAA)}$ was purified from H_2O_2-exposed and unexposed cells by sequential gel and affinity purification. The resulting purified $tRNA^{Leu(CAA)}$ was digested with RNase T1 to give a signature 4-mer oligoribonucleotide harboring either C or m^5C at position 48 (CAAG) (Figure 1A). Additionally, total tRNA from H_2O_2-exposed and unexposed *S. cerevisiae* was digested with RNase U2 to produce another unique 5-mer oligoribonucleotide with C or m^5C at position 34 of $tRNA^{Leu(CAA)}$ (UUCAA) (Figure 1A). As shown in Figure 1B, subsequent mass spectrometric analysis of these oligonucleotides revealed that H_2O_2 exposure caused a 70% increase in m^5C at the wobble position and a 20% decrease at position 48.

m^5C controls the translation of UUG-enriched mRNA

Next we asked if the presence of m^5C in $tRNA^{Leu(CAA)}$ enhanced the translation of UUG-containing mRNA, given the evidence that m^5C at the wobble position of the leucine-inserting amber suppressor $tRNA^{Leu(CUA)}$ enhances translation[21]. To test this hypothesis, we used a dual Renilla and Firefly luciferase reporter construct[42] (illustrated in Figure 2A), in which the linker region connecting these two in-frame coding sequences was either four random or four TTG codons in a row (Control and 4X-TTG, respectively). Expression of the Firefly luciferase portion of the reporter fusion protein is thus dependent upon the efficiency of translating the linker region[42]. The expression of both the Renilla and Firefly luciferase reporters was quantified under conditions of oxidative stress and loss of Trm4 activity (Figures 2B, Supplementary Figure S2). As shown in Figure 2B, loss of Trm4 caused a 9.6-fold reduction in 4X-TTG reporter expression relative to wild-type cells under basal conditions. Following H_2O_2 treatment, there was an even larger 23.8-fold reduction in 4X-TTG reporter activity in *trm4*Δ cells compared to wild-type cells, with 4X-TTG reporter expression in wild-type cells unaffected by H_2O_2 exposure (Figure 2B). Effects of this magnitude were not observed for the control reporter, which was devoid of TTG codons in the linker region (Supplementary Figure S2). The *trm4*Δ cells containing the control reporter had an H_2O_2-induced 2-fold decrease in Firefly luciferase expression, relative to untreated

cells, suggesting contributions by Trm4 to some aspect of general translation during oxidative stress. Taken together, these results are consistent with the idea that translation of TTG-rich sequences is facilitated by Trm4-catalyzed tRNA modifications and that m^5C modifications play an important role in the translational response to H_2O_2 exposure. Coupled with the evidence for H_2O_2-induced increases in m^5C at the wobble position of $tRNA^{Leu(\underline{C}AA)}$, the data support a model in which oxidative stress causes a Trm4-mediated increase in the incorporation of m^5C in $tRNA^{Leu(\underline{C}AA)}$, with the methylated wobble base enhancing the translation of mRNA from genes enriched in TT<u>G</u> codon usage for leucine.

Differential codon enrichment in genes for ribosomal protein paralogs

This direct link between a tRNA wobble modification, codon usage and gene expression immediately raised the question of biases in the distribution of the TTG codon in genes that play a role in responding to oxidative stress. Using a recently developed *S. cerevisiae* codon distribution database[22], we quantified TTG codon use across the yeast genome. An average of 29% of leucines are coded by TTG in the 5782 genes analyzed. However, in 38 genes, more then 90% of the leucines are coded by TTG. Intriguingly, among these 38 genes, 26 encoded ribosomal proteins and the others are loosely related to energy metabolism (Table 1). These 26 ribosomal proteins represent a subset of the 138 such proteins encoded by the yeast genome. Of the 78 proteins that comprise a ribosome in *S. cerevisiae*, 59 occur in homologous pairs, or paralogs, that are believed to have arisen by an evolutionary genome duplication event[23]. Recent evidence supports a model in which individual paralogs play different functional roles in a variety of cell processes in yeast[24–27], with studies by Komili et al. revealing that a specific set of ribosomal protein homologs is necessary for the translation of ASH1 mRNA during bud tip formation[28]. One striking feature of the genes encoding paralogous ribosomal proteins is a bias in frequency of TTG codon use, as shown in Supplementary Tables S1 and S2. For example, 100% and 34% of the leucines in the paralogs Rpl22A and Rpl22B, respectively, are coded by TTG.

H_2O_2 increases a TTG-enriched ribosomal protein paralog

The biased distribution of TTG codons in ribosomal protein paralogs raised another question: will H_2O_2-induced increases in m^5C in $tRNA^{Leu(\underline{C}AA)}$ lead to selective expression of TTG-enriched ribosomal protein paralogs? To test this hypothesis, we used a mass spectrometry-based proteomics approach to determine the relative quantities of several ribosomal protein paralogs in wild-type and *trm4*Δ mutant yeast exposed to H_2O_2[29]. The study entailed isolation of polysomes from lysates of H_2O_2-treated and control yeast cells by differential ultracentrifugation, followed by trypsin digestion of the proteins and quantification of the tryptic peptides by liquid chromatography-coupled high-resolution mass spectrometry (LC-MS). Using this approach, we were able to consistently identify 39 ribosomal proteins in each of three biological replicates (Supplementary Table S3), including seven pairs of distinguishable paralogs (Rpl6a/b, Rpl7a/b, Rpl16a/b, Rpl22a/b, Rpl33a/b, Rpl36a/b, and Rps7a/b) (Supplementary Tables S3, S4). Although the amino acid sequences of each set of paralogous proteins are nearly identical, they contain at least one signature tryptic peptide that could be used to identify and quantify each of 14 ribosomal paralogs in the mixture (Supplementary Table S4). A protein BLAST search in the NCBI database using these peptide sequences confirmed that the peptides were unique to the

specific *S. cerevisiae* ribosomal proteins (data not shown). Further, the sequence identity of these unique peptides was confirmed by the analysis of the b- and y-ion series in collision-induced dissociation (CID) spectra (Supplementary Figure S3).

This approach was applied to determine the relative quantities of ribosomal homologs Rpl22a and Rpl22b, in which 100% and 34% of the leucines were coded by TTG, respectively. In the absence of absolute quantification of individual proteins, changes in the protein levels are expressed as changes in the ratio of the signals for the signature peptides from the protein pairs (e.g., Rpl22a/Rpl22b). The LC-MS signal ratios for the 14 ribosomal paralogs are shown in Supplementary Tables S5 and S6. A comparison of wild-type and *trm4*Δ mutants revealed that loss of *TRM4* caused a significant decrease in the ratio of Rpl22a to Rpl22b and of Rpl16b to Rpl16a (Figure 3), the two sets of paralogs with the largest differences in TTG codon use (Supplementary Table S4). When wild-type and *trm4*Δ cells were exposed to H_2O_2, the ratio of Rpl22a to Rpl22b increased significantly in the wild-type cells but not in the *trm4* mutants (Figure 4). To determine if these changes are indeed occurring at the level of translation, we quantified mRNA for both Rpl22a and Rpl22b by real-time quantitative PCR and we observed that the transcript levels remained unchanged following loss of *TRM4* or exposure to H_2O_2 (Supplementary Table S7).

H_2O_2 enhances translation of proteins with TTG-enriched genes

Having performed a targeted analysis of ribosomal proteins that revealed evidence of selective translation of TTG-enriched proteins, we next undertook a more general proteomic analysis of H_2O_2-induced differences in the ~200 most abundant proteins in yeast (Supplementary Data 1), using a SILAC-based approach to quantify changes in the abundance of proteins in H_2O_2-induced cells[46]. As shown in Figure 5, proteins with high TTG usage are more likely to be down-regulated (Figure 5A, $p = 0.048$ by Student's t-test) as a consequence of loss of Trm4 activity, while these proteins are significantly up-regulated in wild-type cells exposed to H_2O_2 (Figure 5B, $p = 6.41\times10^{-7}$). However, oxidative stress did not affect the expression of proteins from TTG-enriched genes in *trm4*Δ cells (Figure 5C, $p = 0.554$), which is consistent with a role for m^5C in the selective translation of UUG-enriched mRNA species.

Analysis of the functional categories of proteins affected by H_2O_2 exposure (Supplementary Figure S4) reveals that proteins related to translation are significantly up-regulated by oxidative stress, which is consistent with the analysis of ribosomal protein expression in Figure 4, though Rpl22A and Rpl22B could not be differentiated likely as a result of the minimal sequence difference between the two proteins. One interesting complication apparent in Figure 5B is that proteins from genes with intermediate TTG frequencies (i.e., frequencies between the unchanged and up-regulated fractions) are significantly down-regulated in both H_2O_2 exposed wild-type cells ($p = 0.022$) and *trm4*Δ mutants ($p = 0.048$). This illustrates the limitations of our model for selective expression of TTG-enriched genes following oxidative stress and suggests that other layers of translational control are operant in the response to H_2O_2 exposure.

Rpl22A is required for the oxidative stress response in yeast

To further refine the mechanistic link between H_2O_2 exposure, m^5C modification of tRNA, and Rpl22A expression as a survival response, we assessed the H_2O_2 sensitivity of yeast strains lacking individual Rpl16A/B and Rpl22A/B paralogs[29]. As shown in Figure 6 only the loss of *RPL22A* conferred sensitivity to H_2O_2, while the loss of *RPL16A*, *RPL16B* and *RPL22B* did not affect H_2O_2-induced cytotoxicity. The magnitude of the increased cytotoxicity caused by loss of Rpl22A (20% to 10% survival) is similar to the change in cytotoxicity that we observed previously for loss of Trm4[20]. This suggests that Rpl22A contributes significantly to the oxidative stress survival response in yeast. The lack of effect of Rpl16b loss on H_2O_2 toxicity, in spite of the Trm4-dependence of this TTG-enriched paralog (Figure 3), suggests that it shares functional equivalence with Rpl16a in ribosomes.

DISCUSSION

Using a combination of bioanalytical and bioinformatic tools, we have defined a stepwise translational control mechanism responsible for cell survival following oxidative stress, a model for which is shown in Figure 7. While some of the individual steps in this model could be explained by other phenomena, such as tRNA or protein stability, there are few if any alternative mechanisms that could explain the sum of the observed behaviors. The first step in this model involves H_2O_2-induced increases in the level of m^5C at the wobble position of $tRNA^{Leu(\underline{C}AA)}$ (Figure 7A) with a concomitant decrease in m^5C at the neighboring position 48 in the same tRNA. The observation of a 70% increase in the proportion of $tRNA^{Leu(\underline{C}AA)}$ molecules containing a wobble m^5C is consistent with a simple increase in TRM4 activity acting on a fixed concentration of total $tRNA^{Leu(\underline{C}AA)}$. Alternatively, the proportion of m^5C-containing $tRNA^{Leu(\underline{C}AA)}$ could remain constant, with an increase in transcription leading to an increase in the total number of copies of $tRNA^{Leu(\underline{C}AA)}$, or both transcription and TRM4 activity could increase to raise the concentration of $tRNA^{Leu(\underline{C}AA)}$ with m^5C. Finally, given the precedent for stress-induced degradation of tRNA[9,10], oxidative stress could lead to selective degradation of unmethylated $tRNA^{Leu(\underline{C}AA)}$. By any mechanism, the data show that oxidative stress increases the proportion of $tRNA^{Leu(\underline{C}AA)}$ containing m^5C at the wobble position, with an absolute requirement for Trm4 activity for the existence of m^5C[20].

The second step in the model posits that the increase in m^5C in $tRNA^{Leu(\underline{C}AA)}$ enhances the efficiency of translation of mRNAs enriched in the UUG codon recognized by this tRNA (Figure 7B). This is supported by the reporter assay results shown in Figure 2, with loss of Trm4 activity having no or little effect on reporter expression when TTG usage is low but causing a sharp decrease in expression when TTG usage is high. This is consistent with the observation that loss of Trm4, and thus m^5C, decreases the expression of TTG-enriched proteins but not unenriched proteins (Figures 3 and 5). The observation using the unmodified reporter (Supplementary Figure S2) that H_2O_2 exposure of wild-type cells did not affect reporter expression levels, yet it decreased reporter expression in the *trm4*Δ mutant, points to contributions by factors other than modification-specific codon usage in the control of translation during the oxidative stress response.

In addition to the proteome changes shown in Figure 5, the observed changes in expression of ribosomal proteins Rpl22A and Rpl16B (Figures 3 and 4) are consistent with the idea that oxidative stress enhances the translation of UUG-biased mRNAs. The pair of ribosomal gene parologs with the widest difference in the use of TTG for coding leucine, *RPL22A* at 100% and *RPL22B* at 38%, showed the largest changes in protein expression following H_2O_2 exposure, with expression of the high TTG-usage *RPL22A* increasing with oxidative stress and decreasing with loss of *TRM4* (Figure 4). The latter result points to the translational control of Rpl22A by Trm4, with the absolute requirement of oxidation-induced increases in m^5C for the enhanced expression of Rpl22A. While we cannot rule out differential protein stability as a determinant of the proportions of the ribosomal protein paralogs, differences in leucine content do not account for the differential stability of Rpl22A and Rpl22B. The paralogs differ minimally in leucine content and the changes in paralog levels caused by loss of TRM4 do not correlate with this amino acid. While Rpl22A and Rpl22B have 7 and 8 leucines, respectively, and the relative amount of Rpl22A decreases with loss of TRM4, Rpl16A and Rpl16B have 17 and 18 leucines, respectively, yet the relative quantity of RPL16A decreases with loss of TRM4. Further, the data presented here do not provide insights into the function of ribosomes with TTG-enriched ribosomal proteins, such as their potential role in selective translation of mRNAs enriched with TTG or other codons, or their possible role in the early and late stages of the oxidative stress response. A detailed analysis of ribosome-bound mRNAs or nascent peptides in the early and late stages of the oxidative stress response would shed light on these issues. When considered with the other results, our observations suggest that the H_2O_2-induced increase in the level of the Rpl22a ribosomal protein is caused, at least in part, by Trm4-mediated changes in m^5C levels in tRNA with subsequent control of translation of mRNA arising from TTG-enriched genes.

The mechanistic connection between Trm4 and Rpl22A is further established by the observation that loss of either protein makes corresponding *trm4*Δ[20] or *rpl22a*Δ (Figure 6) cells sensitive to H_2O_2. There are parallels for the H_2O_2-sensitive phenotype of *rpl22a*Δ in the recently defined roles of other ribosomal proteins in the oxidative stress response in higher eukaryotes. One example also serves as an illustration of the ribosome filter hypothesis concerning selective translation of mRNA[30]: human ribosomal protein Rpl26 regulates translation of p53, a major node in oxidative stress response[31], by interacting with the 5′-untranslated region of p53 mRNA[32]. Similarly, the highly conserved Rpl22[33] is involved in the activation of internal ribosomal entry site (IRES)-mediated translation in response to several types of stress[34,35] and it participates in murine T-cell development by regulating translation of p53[36]. Interestingly, ribosomal proteins may play roles in stress response other than ribosome structure, as suggested by recent observations of Rpl22 involvement in non-ribosomal ribonucleoprotein complexes such as the telomerase holoenzyme[35,37–39].

This series of observations leads to a model (Figure 7) in which oxidative stress causes an early increase in Trm4-mediated m^5C levels in $tRNA^{Leu(\underline{C}AA)}$, which leads to selective translation of UUG-enriched mRNAs, including ribosomal protein paralog Rpl22a and other proteins derived from many TTG-enriched genes. Clearly, this model does not address the

complexity of translational control mechanisms, as suggested by the proteomic analysis shown in Figure 5, in which mRNA from genes with varying enrichment of TTG codons are not necessarily subject to enhanced translational efficiency. This complexity is further illustrated by the possibility of reprogramming of other modifications, such as H_2O_2-induced increases in Cm and $m^2{}_2G^{20}$, in other tRNA species, with subsequent selective expression of mRNAs enriched with other codons, as well as the potential for reprogramming of ribonucleoside modifications in rRNA species. Nonetheless, the present observations add to the growing recognition of a role for functional diversity in ribosome composition[40] and a role for ribosomes in selective translation of proteins[30]. This reconfiguration of the translation machinery is similar to the proposed generation of "immunoribosomes" as a subset of T-cell ribosomes responsible for translating peptides involved in antigen presentation[41]. The abundance of ribosomal protein paralogs, the variety of RNA modifications in tRNA and rRNA, and the established biases in codon distributions in genes suggest a mechanism capable of fine tuning the translational response to virtually any cell stimulus.

METHODS

Codon reporter assay

The effect of TTG codon frequency on protein expression in wild-type and *trm4*Δ yeast cells was assessed using a dual luciferase reporter system[42] in which Renilla luciferase is connected in-frame to Firefly luciferase by a 12 bp sequence (control: 5′-CCCGGGGAGCTC-3′; or 4X-TTG: 5′-TTGTTGTTGTTG-3′), all under the control of an *ADH1* promoter and *CYC1* terminator[42]. Following transformation with either control or 4X-TTG plasmid, cells were grown to ~5×10^6 cells/mL and then treated with 2 mM H_2O_2 or H_2O for 60 min. Cells pellets were lysed by bead-beating in lysis buffer with and lysates clarified by centrifugation. Luminescence reactions were initiated with Promega DLR (50 μL; Promega; Madison, WI) added to clarified lysates (5 μL) and measured using a Victor Plate Reader (PerkinElmer; Waltham, MA).

RNase digestion of tRNA

Purified tRNALeu$^{(\underline{C}AA)}$ (~2.5 μg) was digested with RNase T1 (1 U; Ambion, Austin, TX) in 10 mM Tris buffer (pH 7.4, 37 °C, 1 hr). RNase U2 (Thermo Scientific, Waltham, MA) digestion (4 U) was carried out using total tRNA (0.5 mg, 37 °C, 4 hr). Oligoribonucleotides were dephosphorylated with alkaline phosphatase (10 U).

Quantifying m^5C in tRNALeu$^{(\underline{C}AA)}$

RNase T1 and U2 digestion maps of tRNA were obtained using the Mongo Oligo Mass Calculator (v2.06; http://library.med.utah.edu/masspec/mongo.htm). Digested tRNA oligos were resolved by HPLC (C18 Hypersil GOLD aQ, 150 × 2.1 mm, 3 μm particle; Thermo Scientific) coupled to a triple quadrupole mass spectrometer (MS) (6410; Agilent Technologies, Foster City, CA) with an electrospray ionization source operated in negative ion mode. HPLC was performed with a gradient of acetonitrile in 8 mM ammonium acetate (0.2 mL/min, 45 °C): 0–2 min, 1%; 2–30 min, 1–15%; 30–31 min, 15–100%; 31–41 min, 100%. MS parameters: drying gas, 325 °C and 8 L/min; nebulizer, 30 psi; capillary voltage,

3800 V; dwell time, 200 ms. The first and third MS quadrupoles were set to unit resolution and the oligos containing m^5C were identified by comparison with standards and CID fragmentation patterns generated in a quadrupole time-of-flight MS. A selected ion chromatogram for a particular charge state of each oligo (unexposed and exposed to H_2O_2) was obtained, and the summation of the mass spectra over a particular peak was used for relative quantification of changes in m^5C levels at positions 34 and 48 of tRNALeu$^{(CAA)}$.

Ribosome isolation

Cells (10^{10}) were resuspended in lysis buffer (10 mL) with 50 mM Tris-acetate, 50 mM ammonium chloride, 12 mM $MgCl_2$, and 1 mM dithiothreitol (pH 7) and lysed mechanically by bead-beating. Cell lysate was centrifuged (10000xg, 10 min), the supernatant collected, and centrifugation repeated twice to remove all particulates. The debris-free supernatant was layered over 2.5 mL of 1 M sucrose, 20 mM HEPES, 500 mM KCl, 2.5 mM magnesium acetate, and 2 mM dithiothreitol at pH 7.4 and centrifuged for 110 min at 370,000xg (r_{max}). Supernatant was removed and the pelleted ribosomes were resuspended in 1.5 mL of a digestion buffer with 100 mM ammonium acetate, pH 8.5. The samples were concentrated by spin dialysis on YM-10 filters. The concentrate was re-diluted with the digestion buffer and subject to spin dialysis five times to remove salts. Yield: ~300 μg of protein.

Identification of ribosomal proteins

As the sequences of ribosomal protein paralogs are similar, we identified a unique tryptic peptide to quantify each paralog. Following reduction with dithiothreitol (1 mM, 2 hr, 37 °C) and alkylation with iodoacetamide (5.5 mM, 30 min, ambient temp.), purified ribosomal proteins (50 μg) were digested with proteomics-grade trypsin (1 μg) in 200 μL of ammonium acetate solution (100 mM, pH 8.5, 37 °C, 12 h). Samples were lyophilized and resuspended in 100 μL of 0.1% formic acid. Peptides in a portion of the tryptic digest (2.5 μg, 5 μL) were analyzed by LC-MS on an Agilent 1200 capillary HPLC coupled to an Agilent 6520 QTOF MS. Peptides were resolved on an Agilent ZORBAX 300SB-C18 column (100 × 0.3 mm, 3 μm particle) eluted with a gradient of acetonitrile in 0.1% formic acid (20 μL/min, 45 °C): 0–25 min, 1–30%; 25–30 min, 30–60%; 30–31 min, 60–95%; 31–36 min, 95%. The MS was operated in positive ion mode with electrospray parameters as follows: fragmentor voltage, 110 V; drying gas, 300 °C and 5 L/min; nebulizer, 20 psi; capillary voltage, 3500 V. Peptide ions were scanned over *m/z* 100–1700 at an acquisition rate of 1.4 spectra/s. Data analysis was performed with Agilent Mass Hunter Software and compounds were detected using Molecular Feature Extractor (MFE) with 300 count minimum peak height and maximum charge state of 2. The MFE compound lists were subjected to peptide mass fingerprint analysis with the Agilent Spectrum Mill proteomics software to identify proteins based upon peptide accurate mass. A search was performed against the NCBInr protein sequence database for *S. cerevisiae* with no protein modifications and missed cleavage considered, and with a 20 ppm mass tolerance and >25% protein coverage.

Identified peptides were sequenced by LC-QTOF using HPLC conditions described earlier and operating the QTOF in targeted MS/MS mode with acquisition rates for both MS and MS/MS scans at 1.4 spectra/s and a constant collision energy of 15 V to selectively monitor ions of the peptides shown in Supplementary Table S4; other MS parameters were described

earlier. Peptide CID spectra were acquired by targeted MS/MS analysis and the band y-ion assignments (Supplementary Figure S3) used to determine the amino acid sequence. A search of the NCBInr protein sequence database confirmed that each peptide uniquely identified its corresponding ribosomal protein paralog. The proteomics data have been deposited in the XX database under the XX accession code.

Relative quantification of ribosomal protein paralogs

With unique tryptic peptides for each paralog (Supplementary Table S4), the selected ion chromatogram of each peptide at charge state +2 was extracted from the total ion chromatogram, with the MS signal intensity determined by summation of the area under the mass spectrum (Supplementary Tables S5, S6). Signal intensities for the ribosomal protein paralogs were normalized by taking their ratio, with the high TTG paralog in the numerator and low TTG in the demoninator (Supplementary Tables S5, S6). This ratio was then used to determine changes in the quantities of ribosomal protein paralogs in H_2O_2-exposed cells (Figures 3, 4).

SILAC proteomics

*Lys1*Δ yeast cells were grown in yeast nitrogen base (YNB) medium containing 30 mg/L of L-lysine-U-[$^{13}C]_6$, [$^{15}N]_2$ (Isotec-SIGMA, Miamisburg, OH) for ≥10 generations, until they reached log-phase (OD_{600} ~ 0.7)[43]. Wild-type and *trm4*Δ yeast cells were grown in YNB medium containing 30 mg/L of L-lysine and were treated with 5 mM H_2O_2 at log-phase[20]. Cells were harvested by centrifugation (1,500×g,10 min, 4 °C), and washed twice with ice-cold H_2O. Cells were lysed by suspension in 2 M NaOH, 8% 2-mercaptoethanol v/v. Following TCA precipitation, proteins were pelleted by centrifugation (15,000×g,15 min, 4 °C) and the pellet was resuspended in 8 M urea, 75 mM NaCl, 50 mM Tris, pH 8.2, 50 mM NaF, 50 mM β-glycerophosphate, 1 mM sodium orthovanadate, 10 mM sodium pyrophosphate, 1 mM PMSF[44]. Protein concentration was determined by the Bradford assay[45]. Heavy SILAC-labeled *lys1*Δ yeast proteins were used as a global internal standard[46]. Following addition of internal standard to all treated and untreated wild-type and *trm4*Δ yeast protein samples (1:1), the protein mixture was reduced in 1mM dithiothreitol (2.5 hr, 37 °C), alkylated with iodoacetamide (5.5 mM, 40 min, ambient temp., dark), and then digested with 50:1 (w/w) trypsin (14 hr, 37 °C).

Peptide mixtures were loaded onto a Vydac C18 trap column (150 μm×10 mm, 5 μm/300 Å particle; Grace, Deerfield, IL) at 5 uL/min and eluted onto a Vydac C18 analytical column (75 μm×150 mm, 5 μm/300 Å particle) at 200 nL/min with a 120 min gradient of 2–98% acetonitrile in 0.1% formic acid. Eluted peptides were analyzed by MS analysis on a QSTAR-XL (Applied Biosystems, Foster City, CA). Acquired MS/MS spectra were parsed by Spectrum Mill and searched against Swiss-Prot database. CID spectra of tryptic peptides were searched against the database sequences within a mass window of 100 ppm for precursor ion searches and 500 ppm for fragment ions. Database search results were filtered based on Spectrum Mill scoring criteria, which include peptide score, a measure of confidence of identification, and scored peak intensity (SPI) that represents the percentage of assigned peaks in CID spectrum. Peptide search results with a score ≥6, SPI ≥60% and no missed cleavages were used for protein quantification. SILAC peptide and protein

quantification was performed with differential expression quantitation and SILAC protein ratios were determined as the average of all peptide ratios assigned to the protein. Differential protein expression was determined by Student's t-test for 4 biological replicates. A summary of identified proteins and their expression levels are presented in Supplementary Data 1.

Gene Ontology annotation

Gene functional categorization and pathway analysis were performed with DAVID Bioinformatics Resources 2011[47]. The annotated proteins are clustered according to the biological process branch of the Gene Ontology (GO) annotation. The statistical significance of over-representation or under-representation of proteins in each GO category was assessed using a hypergeometric distribution and the significance indicated by the *p*-values for each GO category.

Supplementary Material

Refer to Web version on PubMed Central for supplementary material.

Acknowledgments

The authors thank Prof. Wendy Gilbert (Dept. of Biology, MIT) for assistance with ribosome purification. We also thank Drs. Koli Taghizadeh and John Wishnok for assistance with mass spectrometry, which was performed in the Bioanalytical Facilities Core of the MIT Center for Environmental Health Sciences. Financial support was provided by the National Institute of Environmental Health Sciences (ES002109, ES017010, ES015037 and ES017010), the MIT Westaway Fund, a Merck–MIT Graduate Student Fellowship (C.T.Y.C.) and the Singapore-MIT Alliance for Research and Technology.

References

1. Rozenski J, Crain PF, McCloskey JA. The RNA Modification Database: 1999 update. Nucleic Acids Res. 1999; 27:196–197. [PubMed: 9847178]
2. Czerwoniec A, et al. MODOMICS: a database of RNA modification pathways. 2008 update. Nucleic Acids Res. 2009; 37:D118–121. [PubMed: 18854352]
3. Söll, D.; RajBhandary, U. tRNA: Structure, Biosynthesis and Function. ASM Press; 1995.
4. Limbach PA, Crain PF, McCloskey JA. Summary: the modified nucleosides of RNA. Nucleic Acids Res. 1994; 22:2183–2196. [PubMed: 7518580]
5. Agris PF, Vendeix FA, Graham WD. tRNA's wobble decoding of the genome: 40 years of modification. J Mol Biol. 2007; 366:1–13. [PubMed: 17187822]
6. Yarian C, et al. Accurate translation of the genetic code depends on tRNA modified nucleosides. J Biol Chem. 2002; 277:16391–16395. [PubMed: 11861649]
7. Urbonavicius J, Qian Q, Durand JM, Hagervall TG, Bjork GR. Improvement of reading frame maintenance is a common function for several tRNA modifications. EMBO J. 2001; 20:4863–4873. [PubMed: 11532950]
8. Bjork GR, et al. Transfer RNA modification: influence on translational frameshifting and metabolism. FEBS Lett. 1999; 452:47–51. [PubMed: 10376676]
9. Motorin Y, Helm M. tRNA stabilization by modified nucleotides. Biochemistry. 2010; 49:4934–4944. [PubMed: 20459084]
10. Alexandrov A, et al. Rapid tRNA decay can result from lack of nonessential modifications. Mol Cell. 2006; 21:87–96. [PubMed: 16387656]
11. Thompson DM, Parker R. Stressing out over tRNA cleavage. Cell. 2009; 138:215–219. [PubMed: 19632169]

12. Begley U, et al. Trm9-catalyzed tRNA modifications link translation to the DNA damage response. Mol Cell. 2007; 28:860–870. [PubMed: 18082610]
13. Netzer N, et al. Innate immune and chemically triggered oxidative stress modifies translational fidelity. Nature. 2009; 462:522–526. [PubMed: 19940929]
14. Emilsson V, Naslund AK, Kurland CG. Thiolation of transfer RNA in Escherichia coli varies with growth rate. Nucleic Acids Res. 1992; 20:4499–4505. [PubMed: 1383926]
15. Begley TJ, Rosenbach AS, Ideker T, Samson LD. Hot spots for modulating toxicity identified by genomic phenotyping and localization mapping. Mol Cell. 2004; 16:117–125. [PubMed: 15469827]
16. Bennett CB, et al. Genes required for ionizing radiation resistance in yeast. Nat Genet. 2001; 29:426–434. [PubMed: 11726929]
17. Rooney JP, et al. Systems based mapping demonstrates that recovery from alkylation damage requires DNA repair, RNA processing, and translation associated networks. Genomics. 2008; 10:524. [PubMed: 19917080]
18. Kalhor HR, Clarke S. Novel methyltransferase for modified uridine residues at the wobble position of tRNA. Mol Cell Biol. 2003; 23:9283–9292. [PubMed: 14645538]
19. Weissenbach J, Dirheimer G. Pairing properties of the methylester of 5-carboxymethyl uridine in the wobble position of yeast tRNA3Arg. Biochim Biophys Acta. 1978; 518:530–534. [PubMed: 350282]
20. Chan CT, et al. A quantitative systems approach reveals dynamic control of tRNA modifications during cellular stress. PLoS Genetics. 2010; 6:e1001247. [PubMed: 21187895]
21. Strobel MC, Abelson J. Effect of intron mutations on processing and function of Saccharomyces cerevisiae SUP53 tRNA in vitro and in vivo. Mol Cell Biol. 1986; 6:2663–2673. [PubMed: 3537724]
22. Tumu S, Patil A, Towns W, Dyavaiah M, Begley TJ. The Gene Specific Codon Usage Database: A genome-based catalog of one, two, three, four and five codon combinations present in Saccharomyces cerevisiae genes. Database. 2012:bas002. [PubMed: 22323063]
23. Kellis M, Birren BW, Lander ES. Proof and evolutionary analysis of ancient genome duplication in the yeast Saccharomyces cerevisiae. Nature. 2004; 428:617–624. [PubMed: 15004568]
24. Baudin-Baillieu A, Tollervey D, Cullin C, Lacroute F. Functional analysis of Rrp7p, an essential yeast protein involved in pre-rRNA processing and ribosome assembly. Mol Cell Biol. 1997; 17:5023–5032. [PubMed: 9271380]
25. Enyenihi AH, Saunders WS. Large-scale functional genomic analysis of sporulation and meiosis in Saccharomyces cerevisiae. Genetics. 2003; 163:47–54. [PubMed: 12586695]
26. Haarer B, Viggiano S, Hibbs MA, Troyanskaya OG, Amberg DC. Modeling complex genetic interactions in a simple eukaryotic genome: actin displays a rich spectrum of complex haploinsufficiencies. Genes Dev. 2007; 21:148–159. [PubMed: 17167106]
27. Ni L, Snyder M. A genomic study of the bipolar bud site selection pattern in Saccharomyces cerevisiae. Mol Biol Cell. 2001; 12:2147–2170. [PubMed: 11452010]
28. Komili S, Farny NG, Roth FP, Silver PA. Functional specificity among ribosomal proteins regulates gene expression. Cell. 2007; 131:557–571. [PubMed: 17981122]
29. VanDyde, Dervan. Echinomycin binding sites on DNA. Science. 1984; 225:1122–1127. [PubMed: 6089341]
30. Mauro VP, Edelman GM. The ribosome filter redux. Cell Cycle. 2007; 6:2246–2251. [PubMed: 17890902]
31. Liu D, Xu Y. p53, Oxidative Stress, and Aging. Antioxid Redox Signal. 2011; 15:1669–1678. [PubMed: 21050134]
32. Takagi M, Absalon MJ, McLure KG, Kastan MB. Regulation of p53 translation and induction after DNA damage by ribosomal protein L26 and nucleolin. Cell. 2005; 123:49–63. [PubMed: 16213212]
33. Nakao A, Yoshihama M, Kenmochi N. RPG: the Ribosomal Protein Gene database. Nucleic Acids Res. 2004; 32:D168–170. [PubMed: 14681386]

34. Holcik M, Sonenberg N. Translational control in stress and apoptosis. Nat Rev Mol Cell Biol. 2005; 6:318–327. [PubMed: 15803138]
35. Wood J, Frederickson RM, Fields S, Patel AH. Hepatitis C virus 3′X region interacts with human ribosomal proteins. J Virol. 2001; 75:1348–1358. [PubMed: 11152508]
36. Anderson SJ, et al. Ablation of ribosomal protein L22 selectively impairs alphabeta T cell development by activation of a p53-dependent checkpoint. Immunity. 2007; 26:759–772. [PubMed: 17555992]
37. Dobbelstein M, Shenk T. In vitro selection of RNA ligands for the ribosomal L22 protein associated with Epstein-Barr virus-expressed RNA by using randomized and cDNA-derived RNA libraries. J Virol. 1995; 69:8027–8034. [PubMed: 7494316]
38. Le S, Sternglanz R, Greider CW. Identification of two RNA-binding proteins associated with human telomerase RNA. Mol Biol Cell. 2000; 11:999–1010. [PubMed: 10712515]
39. Toczyski DP, Steitz JA. EAP, a highly conserved cellular protein associated with Epstein-Barr virus small RNAs (EBERs). EMBO J. 1991; 10:459–466. [PubMed: 1846807]
40. Dlakic M. The ribosomal subunit assembly line. Genome Biol. 2005; 6:234. [PubMed: 16207363]
41. Yewdell JW, Nicchitta CV. The DRiP hypothesis decennial: support, controversy, refinement and extension. Trends Immunol. 2006; 27:368–373. [PubMed: 16815756]
42. Plant EP, et al. Differentiating between near- and non-cognate codons in Saccharomyces cerevisiae. PLoS One. 2007; 2:e517. [PubMed: 17565370]
43. de Godoy LM, et al. Comprehensive mass-spectrometry-based proteome quantification of haploid versus diploid yeast. Nature. 2008; 455:1251–1254. [PubMed: 18820680]
44. Gruhler A, et al. Quantitative phosphoproteomics applied to the yeast pheromone signaling pathway. Mol Cell Proteomics. 2005; 4:310–327. [PubMed: 15665377]
45. Bradford MM. A rapid and sensitive method for the quantitation of microgram quantities of protein utilizing the principle of protein-dye binding. Anal Biochem. 1976; 72:248–254. [PubMed: 942051]
46. Ishihama Y, et al. Quantitative mouse brain proteomics using culture-derived isotope tags as internal standards. Nat Biotechnol. 2005; 23:617–621. [PubMed: 15834404]
47. Huang da W, Sherman BT, Lempicki RA. Systematic and integrative analysis of large gene lists using DAVID bioinformatics resources. Nat Protoc. 2009; 4:44–57. [PubMed: 19131956]

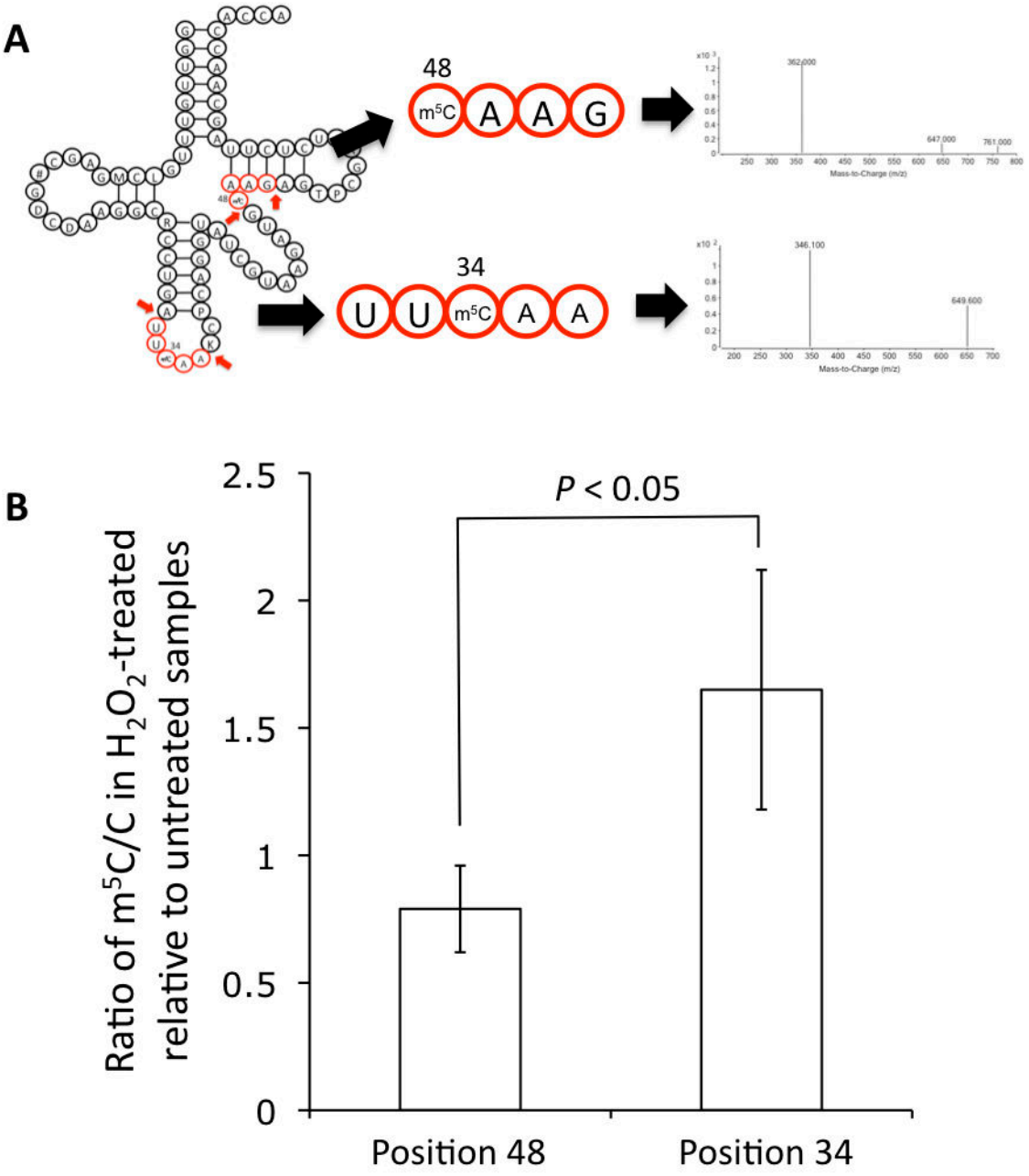

Figure 1.

H_2O_2 exposure increases the level of m^5C at the wobble position of $tRNA^{Leu(\underline{C}AA)}$. (**A**) $tRNA^{Leu(\underline{C}AA)}$ was digested with ribonucleases to generate oligoribonucleotides containing m^5C or C at position 34 (CAAG) or position 48 (UUCAA), and the oligoribonucleotides were quantified by mass spectrometry. (**B**) The graph shows the ratio of m^5C/C in $tRNA^{Leu(\underline{C}AA)}$ from H_2O_2-treated cells relative to untreated cells. The data represent mean ± SD for three experiments. The data for position 34 are significantly different from those for position 48 by Student's t-test with $p < 0.05$.

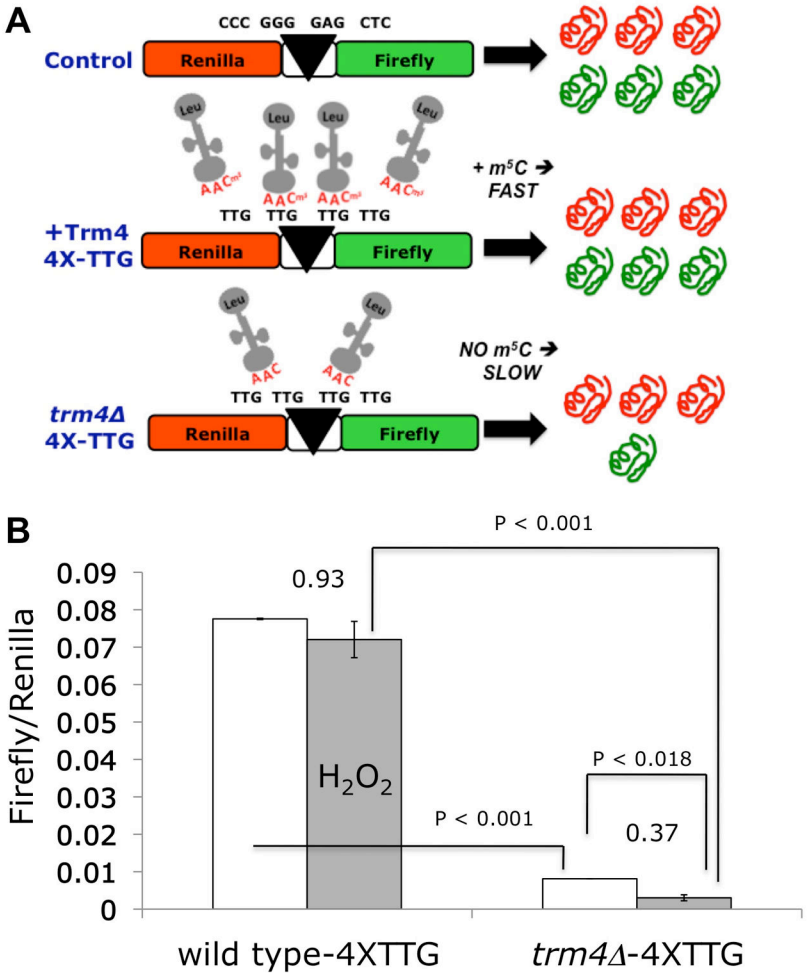

Figure 2.

H_2O_2 and Trm4 methyltransferase control gene expression at the level of TTG codon usage. (**A**) Scheme illustrating the dual luciferase reporter system for assessing the effect of TTG codon usage on protein expression in wild-type and *trm4*Δ mutant yeast cells transformed with either control or 4X-TTG reporter plasmids. (**B**) Control and 4X-TTG reporter activity was quantified in H_2O_2-exposed (gray bars) and unexposed (white bars) wild-type or *trm4*Δ cells. The ratio of treated to untreated is indicated above each condition. Data represent mean ± deviation about the mean for three biological replicates.

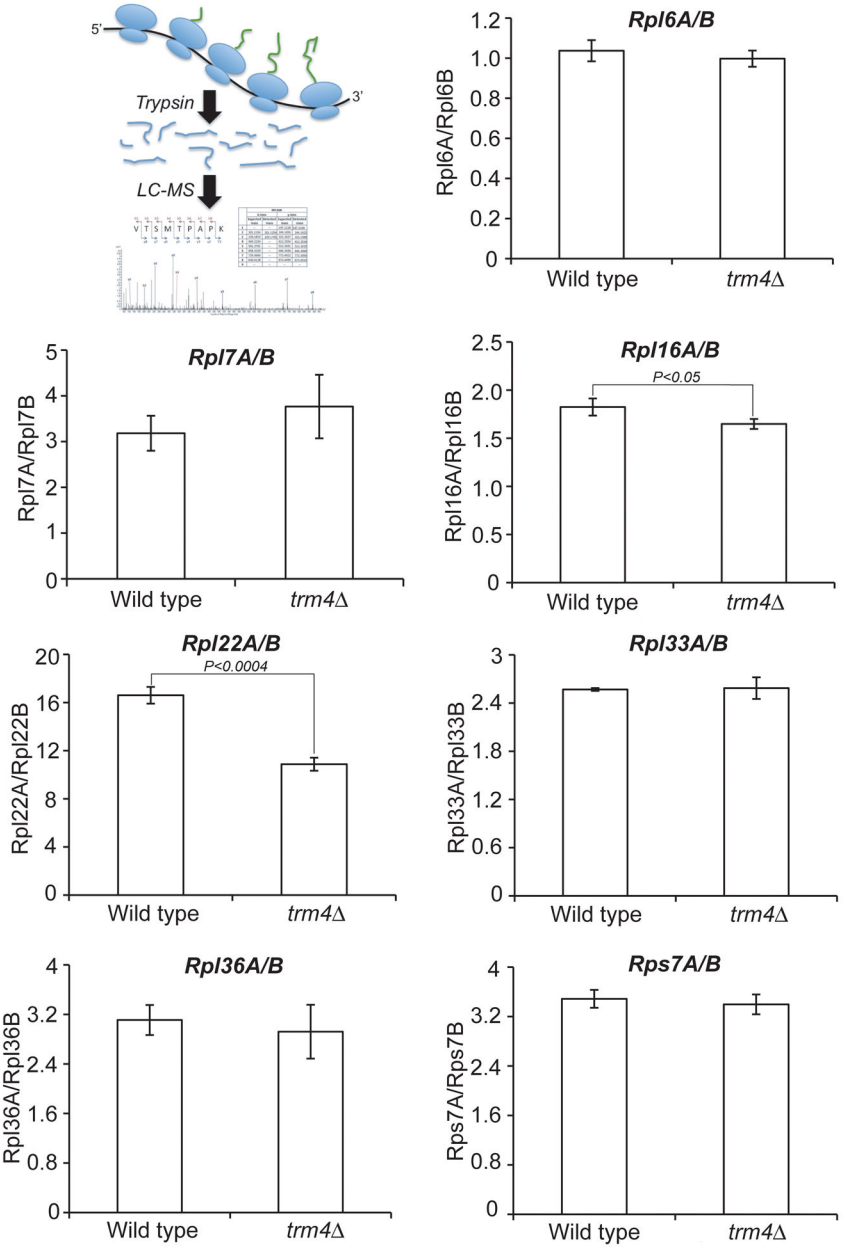

Figure 3.

Loss of Trm4 methyltransferase decreases the proportion of ribosomes containing TTG codon-enriched ribosomal protein paralogs. Ribosomal proteins in wild-type and *trm4*Δ mutant *S. cerevisiae* were quantified by LC-MS/MS (schematic inset) and the relative quantities of ribosomal protein paralogs presented as the ratio of the signal intensity for the paralog with high TTG-usage to that of the low-usage paralog. Data represent mean ± SD for three biological replicates. *p* values denote statistically significant differences by Student's t-test.

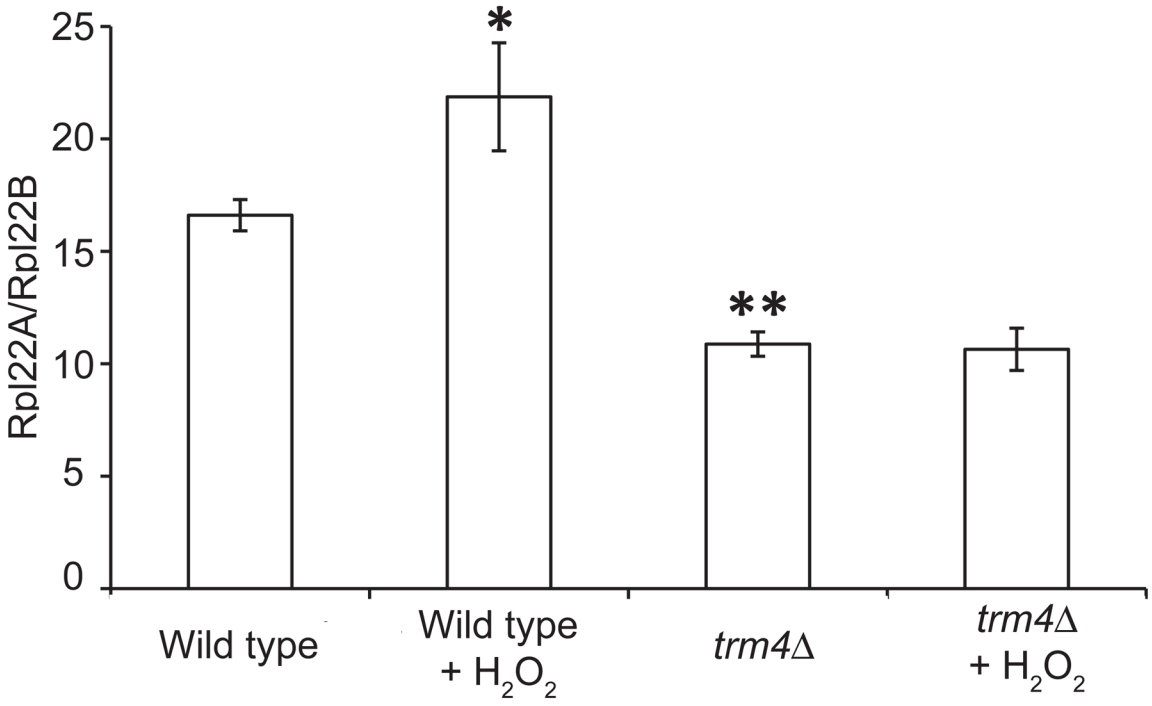

Figure 4.

H_2O_2 exposure increases the proportion of ribosomes containing ribosomal protein paralog Rpl22a in wild-type *S. cerevisiae* but not *trm4*Δ mutants. Cells were exposed to 2 mM H_2O_2 for 1 hr and the quantities of ribosomal proteins were determined by LC-MS/MS analysis. Data are expressed as the ratio of the TTG-enriched paralog Rpl22a to unenriched Rpl22b. Data represent mean ± SD of three biological replicates. Asterisks denote statistically significant differences between H_2O_2-treated and untreated cells as judged by Student's t-test with $p < 0.05$.

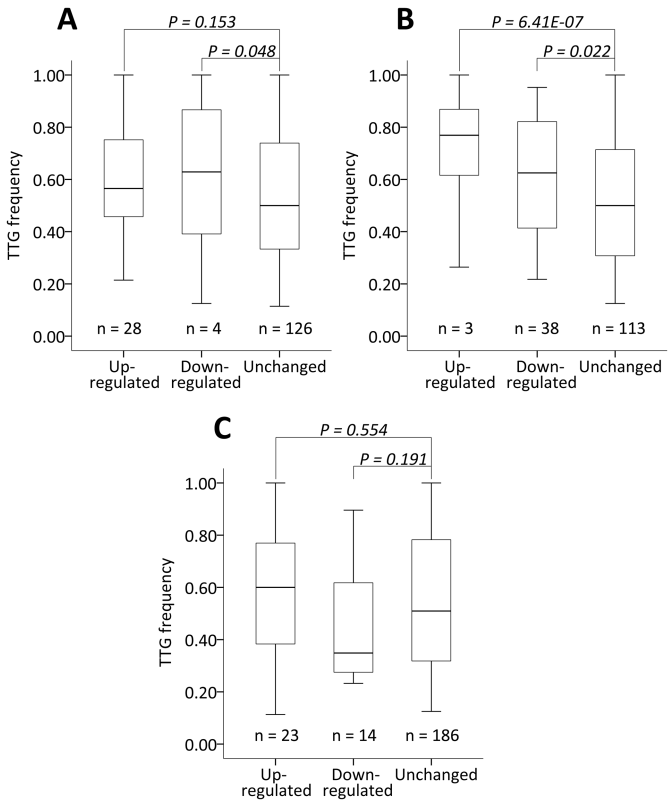

Figure 5.

SILAC-based proteomic analysis reveals that H_2O_2 enhances the translation of TTG-enriched proteins. Protein extracts from control and H_2O_2-treated wild-type and *trm4* mutant yeast were mixed 1:1 with proteins from U-[^{13}C,^{15}N]-lysine-labeled *lys1*Δ yeast cells as an internal standard[46]. Protein mixtures were then subjected to trypsin digestion and proteomic analysis by LC-QTOF analysis. The quantities of the 261 most abundant proteins appearing in each of four biological replicates were analyzed by Student's t-test (p <0.05) for increased (up-regulation), decreased (down-regulation) or unchanged levels in H_2O_2-treated versus control cells, or wild-type versus *trm4*Δ mutant. Within these three groups of proteins, the frequency of using TTG to code for leucine was calculated. The resulting frequency data are presented as a box-and-whiskers plot with the bar representing the median value, the box encompassing the range of data between the first and third quartile, and the error bars embracing data within 1.5-times interquartile range. Differences between up-regulated, down-regulated and unchanged categories were subjected to Student's t-test with the indicated p values.

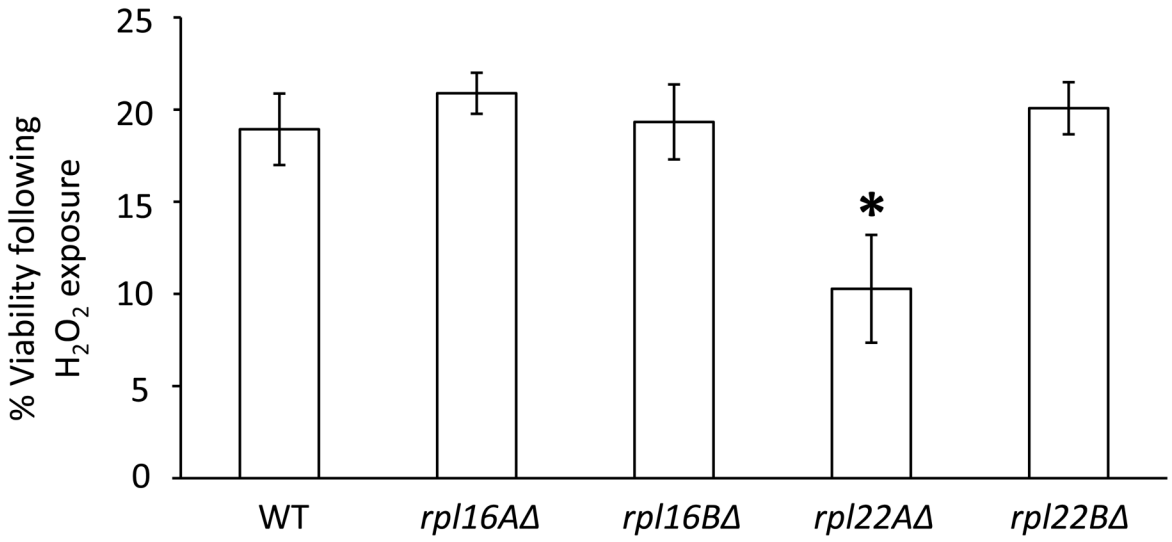

Figure 6.

Ribosomal protein paralog Rpl22a confers resistance to H_2O_2 exposure in *S. cerevisiae*. Wild-type *S. cerevisiae* and strains lacking *RPL16A*, *RPL16B*, *RPL22A*, or *RPL22B* were exposed to 5 mM H_2O_2 and survival was assayed as described in Methods. Data represent mean ± SD of three biological replicates. The asterisk denotes a statistically significant difference compared to all other values in the figure, as judged by Student's t-test with $p < 0.05$.

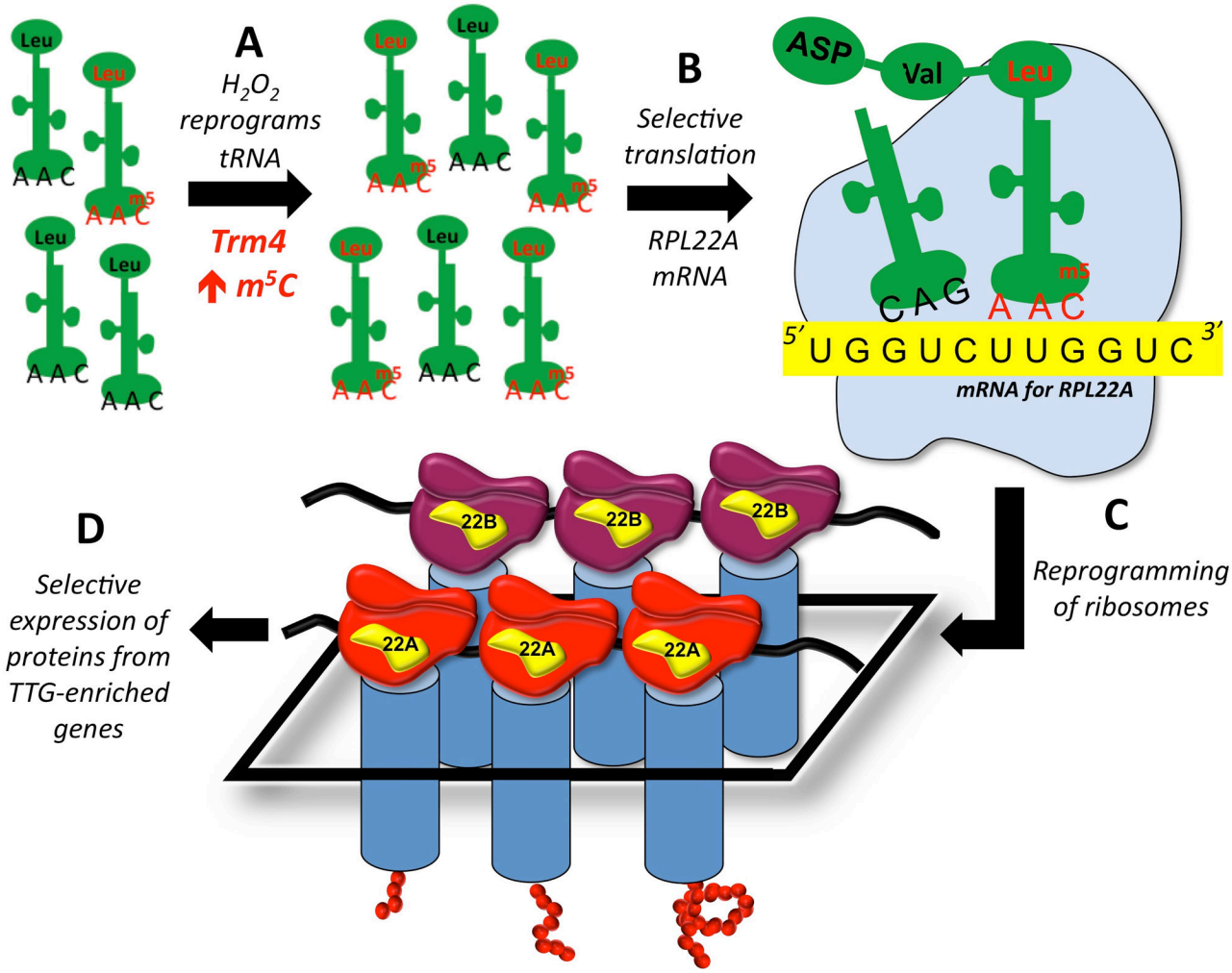

Figure 7.

Proposed mechanism by which increase in m^5C level regulates translation of ribosomal protein paralogs and confers resistance to H_2O_2. Exposure to H_2O_2 leads to an elevation in the level of m^5C at the wobble position of the leucine tRNA for translating the codon UUG on mRNA (**A**), which enhances the translation of the UUG-enriched *RPL22A* mRNA relative to its paralog *RPL22B* (**B**) and leads to changes in ribosome composition (**C**). This reprogramming of tRNA and ribosomes ultimately causes selective translation of proteins from genes enriched with the codon TTG.

Table 1

S. cerevisiae genes with ≥ 90% TTG codon usage for leucine.

Gene Name	#TTG	Freq. of TTG[1]	Protein Function
RPL15A	13	1	Protein component of the large (60S) ribosomal subunit
RPL28	9	1	Ribosomal protein of the large (60S) ribosomal subunit
RPL39	2	1	Protein component of the large (60S) ribosomal subunit
RPS10B	9	1	Protein component of the small (40S) ribosomal subunit
CCW12	9	1	Cell wall mannoprotein
RPL22A	7	1	Protein component of the large (60S) ribosomal subunit
RPL43A	3	1	Protein component of the large (60S) ribosomal subunit
RPL37B	2	1	Protein component of the large (60S) ribosomal subunit
RPL37A	2	1	Protein component of the large (60S) ribosomal subunit
HYP2	11	1	Translation elongation factor eIF-5A
RPS15	9	1	Protein component of the small (40S) ribosomal subunit
RPL36B	6	1	Protein component of the large (60S) ribosomal subunit
NOP10	5	1	Constituent of small nucleolar ribonucleoprotein particles
RPS26B	4	1	Protein component of the small (40S) ribosomal subunit
HSP12	3	1	Plasma membrane localized protein
TDH3	20	0.95	Glyceraldehyde-3-phosphate dehydrogenase, isozyme 3
TDH2	20	0.95	Glyceraldehyde-3-phosphate dehydrogenase, isozyme 2
TDH1	19	0.95	Glyceraldehyde-3-phosphate dehydrogenase, isozyme 1
RPL8A	19	0.95	Ribosomal protein L4 of the large (60S) ribosomal subunit
RPS6B	19	0.95	Protein component of the small (40S) ribosomal subunit
RPS6A	19	0.95	Protein component of the small (40S) ribosomal subunit
RPL10	16	0.94	Protein component of the large (60S) ribosomal subunit
RPL4A	26	0.93	Protein component of the large (60S) ribosomal subunit
RPL4B	26	0.93	Protein component of the large (60S) ribosomal subunit
RPS13	13	0.93	Protein component of the small (40S) ribosomal subunit
RPS5	13	0.93	Protein component of the small (40S) ribosomal subunit
ENO2	35	0.92	Enolase II
ANB1	11	0.92	Translation elongation factor eIF-5A
CDC19	32	0.91	Pyruvate kinase
RPL12B	10	0.91	Protein component of the large (60S) ribosomal subunit
PDC1	49	0.91	Major of three pyruvate decarboxylase isozymes
RPS2	19	0.90	Protein component of the small (40S) subunit
RPL8B	19	0.90	Ribosomal protein L4 of the large (60S) ribosomal subunit
ENO1	36	0.90	Enolase I
RPL17A	9	0.90	Protein component of the large (60S) ribosomal subunit
RPL17B	9	0.90	Protein component of the large (60S) ribosomal subunit

Gene Name	#TTG	Freq. of TTG[1]	Protein Function
RPS9B	18	0.90	Protein component of the small (40S) ribosomal subunit
RPL9A	9	0.90	Protein component of the large (60S) ribosomal subunit

[1] Proportion of leucines encoded by TTG